

# Rapid retraction of microvolume aqueous plugs traveling in a wettable capillary

 Jinho Kim,<sup>1</sup> John D. O'Neill,<sup>1</sup> and Gordana Vunjak-Novakovic<sup>1,2,a)</sup>
<sup>1</sup>Department of Biomedical Engineering, Columbia University, New York, New York 10027, USA

<sup>2</sup>Department of Medicine, Columbia University, New York, New York 10032, USA

(Received 15 July 2015; accepted 29 September 2015; published online 7 October 2015)

We report a transport behavior—specifically, rapid retraction movement—of small ( $\sim\mu\text{L}$ ) deionized water plugs traveling in series within a small wettable tubular geometry. In this study, two water plugs separated by a certain distance in a dry cylindrical glass capillary were moved by positive pressure airflow applied at the tube inlet. As the plugs travel, a thin aqueous film is generated between the plugs as a result of the leading plug's aqueous deposition onto the inner surface of the tube. The leading plug continuously loses volume by film deposition onto the surface and eventually ruptures. Then, the lagging plug quickly travels the distance initially separating the two plugs (plug retraction). Our studies show that the rapid retraction of the lagging plug is caused by surface tension in addition to the positive pressure applied. Furthermore, the plug retraction speed is strongly affected by tube radius and the distance between the plugs. © 2015 AIP Publishing LLC. [<http://dx.doi.org/10.1063/1.4932956>]

Surface tension can produce sufficient energy to promote the flow and movement of small objects (length scale: 1 mm).<sup>1,2</sup> For example, shorebirds feed on prey suspended in water droplets by employing surface tension forces to propel the droplets into their mouths by repeatedly opening and closing their beaks.<sup>3</sup> Droplet motion is enabled by the surface tension forces generated by contact-angle hysteresis, i.e., the difference in the contact angles between the droplet's advancing and receding menisci within the bird's beak.

Alternatively, because the surface tension of liquids is temperature-dependent, the position of a liquid droplet can be manipulated by generating a surface tension gradient across the droplet via localized heating.<sup>4,5</sup> Additionally, flow transport within small geometries such as pores and microchannels can be greatly affected by surface energy. In crude oil recovery, for example, the rate of oil extraction from subterranean reservoirs is strongly affected by surface energy in combinatory interactions between oil and surrounding porous media such as soil and rock.<sup>6,7</sup>

Recent studies have demonstrated that small liquid plugs traveling in series through a microchannel network can rapidly move when preceding plugs rupture.<sup>8,9</sup> Such a flow transport phenomenon, which is induced by surface tension, can be observed in many fluidic processes including the clearance of mucus plugs in the pulmonary airways.<sup>10,11</sup> Understanding the subtle physical mechanism of the rapid plug movement would enhance the ability to manipulate small volumes of liquid for desired applications; however, a better understanding of this fluid transport behavior requires additional rigorous investigation.

In this letter, we present experimental and theoretical analyses for rapid retraction of small ( $\sim\mu\text{L}$  volume) water plugs traveling in a wettable glass capillary. Plug retraction was induced when the leading of two liquid plugs moving in

series in a glass capillary ruptured due to a critical loss of volume by deposition of a thin aqueous film onto the dry wall of the tube. We show that the rupture of the leading plug causes rapid movement of the lagging plug (plug retraction). Our analysis indicates that the surface tension between the two plugs (initially connected by a thin aqueous film) and the positive pressure applied to induce plug movement are responsible for the abrupt plug movement. Furthermore, we confirmed experimentally that the inner diameter of the capillary as well as the distance between the plugs—which we believe to be the two most important length scales for this flow phenomenon—can strongly affect plug retraction behavior.

Figure 1(a) shows schematically the retraction behavior of a water plug in a glass capillary. When positive air

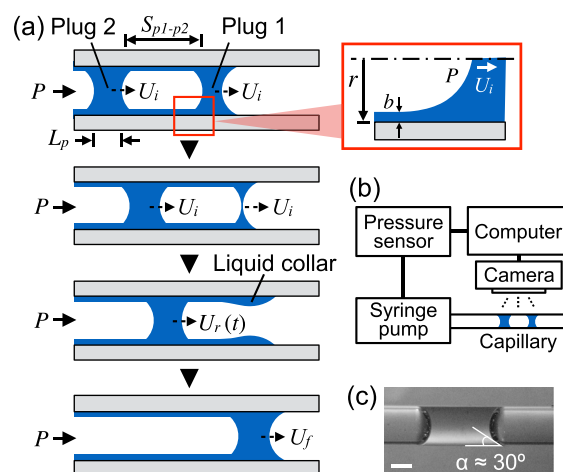


FIG. 1. Schematic of water plug transport and retraction in a wettable tube, and measurement setup. (a) Schematic depiction of water plug transport and retraction of the lagging plug (Plug 2) due to rupture of the leading plug (Plug 1) in a cylindrical glass capillary. Inset: Sketch of thin liquid film deposition by Plug 1 on the tube inner surface. (b) Experimental setup for the plug retraction study. (c) Photograph of a water plug placed in a glass tube with the static contact angle  $\alpha \approx 30^\circ$ . Scale bar: 500  $\mu\text{m}$ .

<sup>a)</sup>Author to whom correspondence should be addressed. Electronic mail: gv2131@columbia.edu.

pressure  $P$  is applied via airflow at the inlet of a glass tube (inner radius  $r$ ) containing two small water plugs (Plug 1 and Plug 2) with interdistance  $S_{p1-p2}$ , both plugs travel at an initial speed  $U_i$  in the same direction. As the plugs continue to travel, the length  $L_{p1}$  of the leading plug (Plug 1) decreases due to the deposition of a thin water film with thickness  $b \sim rCa_p^{2/3}$  on the inner surface of the capillary if  $Ca_p \ll 1$ , where  $Ca_p = \mu U_i / \sigma$  is the capillary number of the plug, and  $\mu$  and  $\sigma$  are the viscosity and surface tension of water, respectively.<sup>12,13</sup> When the volume of Plug 1 is significantly reduced, the plug eventually ruptures and remains as a collar on the tube wall. As soon as Plug 1 ruptures, the speed of the leading plug (Plug 2) rapidly increases and quickly travels the distance  $S_{p1-p2}$ . We define “plug retraction” as the rapid movement of a plug in this letter. During plug retraction, the speed of Plug 2 continues to decrease from the maximum speed  $U_{max}$  to a final speed  $U_f$  because of viscous friction exerted from the wall surface. Thus, the speed of Plug 2 during the retraction can be  $U_r(t) = (U_{max} - U_f)e^{-t/\tau} + U_f$ , where  $\tau = \rho r^2 / 8\mu$  is the time constant and  $\rho$  is the density of water.<sup>14</sup>

Following the rupture of Plug 1, the speed  $U_{max}$  of Plug 2 can be obtained from the conservation of momentum equation  $d(MU_{max})/dt = \sum F$ , where  $M$  is the mass of Plug 2 and  $\sum F$  is the sum of the forces acting on the plug. Since the Reynolds, Bond, and capillary numbers of plugs in this study are, respectively,  $Re = 2r\rho U_{max}/\mu \gg 1$ ,  $Bo = 4\rho g r^2/\sigma \ll 1$ , and  $Ca_p = \mu U_{max}/\sigma \ll 1$ , the motion of Plug 2 could be driven by surface tension in addition to the applied pressure, with inertia accounting for the the major resistance to plug motion during retraction. Thus, with the mass flux of the liquid plug  $dM/dt \sim \rho A U_{max}$ , we obtain  $U_{max} \sim [(\sigma/L_c + P_r)/\rho]^{1/2}$ , where  $A$  is the cross-sectional area of the plug,  $P_r$  is the pressure involving plug retraction, and  $L_c$  is the characteristic length. As we show here,  $L_c$  is related to  $S_{p1-p2}$  and  $r$ . In fact, on a flat surface wetted with precursor liquid, the velocity of droplets migrating by surface tension scales with distance between the droplets.<sup>15,16</sup> Notably, for a rupturing soap bubble,  $L_c$  scales with bubble thickness,<sup>17</sup> while for retracting liquid puddles on non-wetting substrates,  $L_c$  is proportional to the puddle width.<sup>18</sup>

A schematic of the experimental setup is shown in Fig. 1(b). Clean, dry glass capillary tubes ( $r = 300 \mu\text{m}$ ,  $450 \mu\text{m}$ , and  $750 \mu\text{m}$ , Vitrotubes<sup>TM</sup>, VitroCom) were prepared for the experiments. Then, a small volume (Plug 1,  $Vol_{p1} = 0.5 \mu\text{l}$ ) of deionized (DI) water ( $\rho = 1000 \text{ kg/m}^3$ ,  $\mu = 10^{-3} \text{ Ns/m}^2$ , and  $\sigma = 72 \text{ mN/m}$ )<sup>14</sup> was introduced through one end of the capillary using a micropipette. The plug was then moved a certain distance to create a plug interdistance  $S_{p1-p2}$  by infusing air (flow rate  $Q < 0.1 \text{ ml/min}$ ) with a syringe pump (GenieTouch Syringe Pump, Kent Scientific), which was connected to the capillary via polymer tubing (Masterflex, Cole-Parmer). After carefully detaching the polymer tubing from the capillary, another plug (Plug 2,  $Vol_{p2} = 0.5\text{--}2 \mu\text{l}$ ) was introduced through the same end of the capillary using a micropipette. To move both plugs simultaneously, the polymer tubing was reconnected to the capillary and air was infused ( $Q = 0.05\text{--}1.5 \mu\text{l/min}$ ) using the syringe pump to achieve various plug capillary numbers ( $Ca_p = 1.8 \times 10^{-5}\text{--}5.5 \times 10^{-4}$ ). The pressure  $P$  applied at the

capillary inlet was measured using a pressure sensor (MPXV7002GC6U, Freescale Semiconductor) connected to a computer. Videos of the plugs traveling through the capillary were recorded using a digital camera (Nikon J1, Nikon) and analyzed using ImageJ software (NIH). In this study, plug volume  $Vol_p$  was  $0.5 \mu\text{l}$ , unless otherwise specified. To maintain consistent interfacial tension between glass capillary and water plugs, the capillary was cleaned thoroughly before each experiment by flowing  $300 \mu\text{l}$  fresh DI water at  $Q = 100 \mu\text{l/s}$  and then by blowing dry air through the capillary for 1 min. Figure 1(c) shows a water plug formed in a glass tube with the static contact angle  $\alpha \approx 30^\circ$ .

Representative images obtained at different times and locations during transport of two water plugs in a glass tube ( $r = 450 \mu\text{m}$ ,  $S_{p1-p2} = 1 \text{ cm}$ ) are shown in Fig. 2(a). When airflow ( $Q = 0.5 \text{ ml/min}$ ,  $Ca_p = 1.82 \times 10^{-4}$ ) was introduced to the capillary at  $t = 0 \text{ s}$ , both plugs started to move at an initial speed  $U_i = 1.2 \text{ cm/s}$ , maintaining a constant  $S_{p1-p2}$ . At  $t = 4.03 \text{ s}$ , Plug 1 ruptured after traveling  $4.9 \text{ cm}$ . Simultaneously, Plug 2 rapidly traveled  $S_{p1-p2}$  to the location where Plug 1 ruptured within  $0.2 \text{ s}$ , at an average retraction speed  $U_r^* = 5 \text{ cm/s}$ . Interestingly, at  $t = 4.23 \text{ s}$  the length of Plug 2  $L_{p2}$  increased 15% compared to its initial length just before plug retraction because it picked up some of the residual volume that Plug 1 had deposited on the inner surface of the tube. Plug 2 continued to travel an additional  $6.5 \text{ cm}$  until it ruptured at  $t = 9.75 \text{ s}$ .

We investigated the effect of the plug interdistance  $S_{p1-p2}$  on the speed of Plug 2 during plug retraction ( $Ca_p = 1.82 \times 10^{-4}$ ). Increased overall speeds of Plug 2 (i.e.,  $dU_r = U_r^* - U_i$ ) were determined for various plug interdistances ( $S_{p1-p2} \sim 1\text{--}3 \text{ cm}$ ) and tube sizes ( $r = 300, 450$ , and  $750 \mu\text{m}$ ). As shown in Fig. 2(b),  $dU_r$  was strongly affected

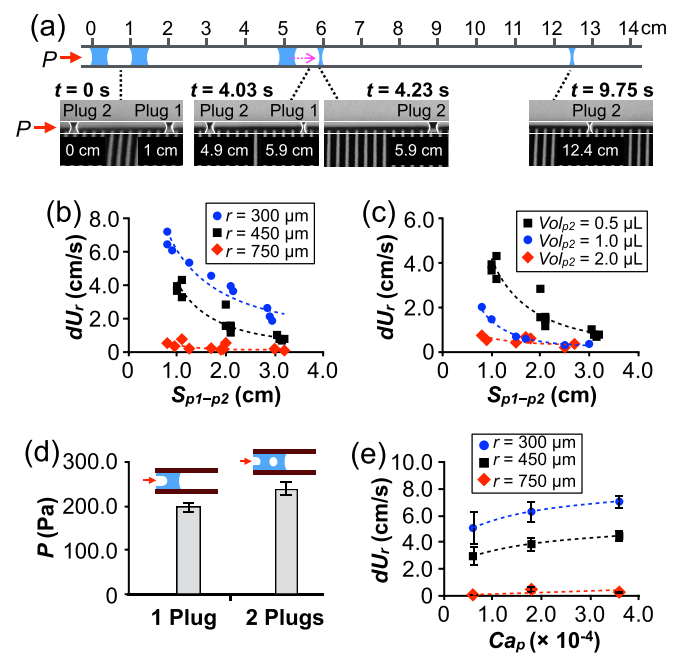


FIG. 2. Measurements of plug travel speed and pressure during plug retraction. (a) Images obtained at different times and locations in a glass capillary during transport of Plug 1 and Plug 2. Each grid is 1 mm. (b)  $dU_r$  of Plug 2 measured with various  $S_{p1-p2}$  and  $r$ , and (c) with various  $Vol_{p2}$ . (d)  $P$  measured for water plugs moving through a glass tube. (e)  $dU_r$  of Plug 2 measured with various  $Ca_p$  in tubes with different  $r$ .

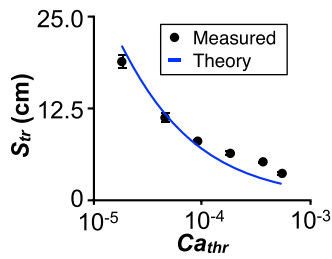


FIG. 3.  $S_{tr}$  measured against various  $Ca_{thr}$  in a glass capillary ( $r = 300 \mu\text{m}$ ). Theory:  $S_{tr} = Vol_{dep} / (k\pi r^2 Ca_{thr}^{2/3})$  with  $k = 5.4$ .

by the interdistance for a given tube size, as  $dU_r$  generally increased with decreasing  $S_{p1-p2}$ . However, while  $dU_r$  was greater than 7 cm/s with shorter plug interdistance in a smaller tube (e.g.,  $S_{p1-p2} = 1 \text{ cm}$ ,  $r = 350 \mu\text{m}$ ),  $dU_r$  was very small ( $< 0.5 \text{ cm/s}$ ) and less affected by  $S_{p1-p2}$  in a larger tube (e.g.,  $r = 750 \mu\text{m}$ ). Surface tension became less significant as the plug volume increased, as shown in Fig. 2(c). As  $Vol_{p2}$  increased,  $dU_r$  became smaller in a tube ( $r = 450 \mu\text{m}$ ,  $Ca_p = 1.82 \times 10^{-4}$ ,  $S_{p1-p2} \sim 1\text{--}3 \text{ cm}$ ) due to the influence of gravity with increasing plug volume. For example,  $dU_r \sim 4 \text{ cm/s}$  and  $\sim 0.6 \text{ cm/s}$  for  $Vol_{p2} = 0.5 \mu\text{l}$  and  $2 \mu\text{l}$ , respectively, when  $S_{p1-p2} \sim 1 \text{ cm}$ .

Figure 2(d) shows air pressure  $P$  measured at the tube inlet as one and two plugs were pushed through a glass tube ( $Ca_p = 1.82 \times 10^{-4}$ ,  $r = 300 \mu\text{m}$ ). Approximately 198 Pa was required to move one plug, while  $\sim 238 \text{ Pa}$ , nearly 20% greater pressure, was needed for two plugs because of the increased number of menisci (from 2 menisci in 1 plug to 4 menisci in 2 plugs), which introduced greater resistance to plug movement.<sup>19</sup> The difference between pressures for one and two plugs indicated that some of the excess pressure  $P_r$  could be involved in plug retraction when one of two plugs (i.e., Plug 1) suddenly ruptured within less than a millisecond.<sup>17</sup> To examine the effect of pressure, we measured  $dU_r$ ,

of Plug 2 with various airflow rates used to generate  $P$  in this study, resulting in different plug capillary numbers ( $Ca_p = 0.6 \times 10^{-4}$ ,  $1.82 \times 10^{-4}$ ,  $3.64 \times 10^{-4}$ ) in tubes ( $r = 300 \mu\text{m}$ ,  $450 \mu\text{m}$ ,  $750 \mu\text{m}$ ). As shown in Fig. 2(e),  $dU_r$  generally increased with  $Ca_p$  and was greater in smaller tubes. In larger tubes,  $dU_r$  became much smaller because of the reduced significance of surface tension, as  $dU_r$  was at least 30 times smaller in  $r = 750 \mu\text{m}$  than in  $r = 300 \mu\text{m}$  for the  $Ca_p$  tested.

When two small plugs of liquid travel in a dry circular tube, they wet the inner surface of the tube. As they move, the threshold plug capillary number  $Ca_{thr}$  can be estimated.  $Ca_{thr}$  is a number below which the leading plug is not exhausted by deposition and therefore does not rupture. Thus, both plugs can travel a specified distance at the same speed while maintaining a constant interdistance. The liquid volume deposited on the tube surface is  $Vol_{dep} = kb\pi r S_{tr}$ , where  $b$ ,  $k$ ,  $Vol_{dep}$ , and  $S_{tr}$  are, respectively, uniform film thickness, a constant, liquid volume deposited, and plug travel distance. Thus, if  $Ca_p \ll 1$ , we obtain  $S_{tr} = Vol_{dep} / (k\pi r^2 Ca_{thr}^{2/3})$ . As an example,  $Ca_{thr}$  for a water plug ( $Vol_p = 0.5 \mu\text{l}$ ) traveling in a glass tube ( $r = 450 \mu\text{m}$ ) was experimentally measured for various  $S_{tr}$  and is shown in Fig. 3 with theoretically calculated values for  $k = 5.4$ . In general, smaller  $Ca_{thr}$  is expected for greater  $r$  and longer  $S_{tr}$ , suggesting that plugs should be moved slower to travel a longer distance in a larger tube.

Using high-speed imaging, we conducted a detailed study on the travel speed  $U_r(t)$  and length  $L_{p2}$  of Plug 2 during plug retraction in a glass tube ( $r = 450 \mu\text{m}$ ,  $S_{p1-p2} = 1.2 \text{ cm}$ ,  $Ca_p = 1.82 \times 10^{-4}$ ). Figures 4(a) and 4(b) show, respectively, consecutive images obtained from a video recorded at 400 frames per second and the trajectory of Plug 2 during plug retraction for 0.25 s (Arrows: the location at which Plug 1 ruptured). As shown, Plug 2 initially traveled a longer distance  $S_{tr}$ , indicating the plug very rapidly reached its maximum speed just after Plug 1 ruptured. Figure 4(c)

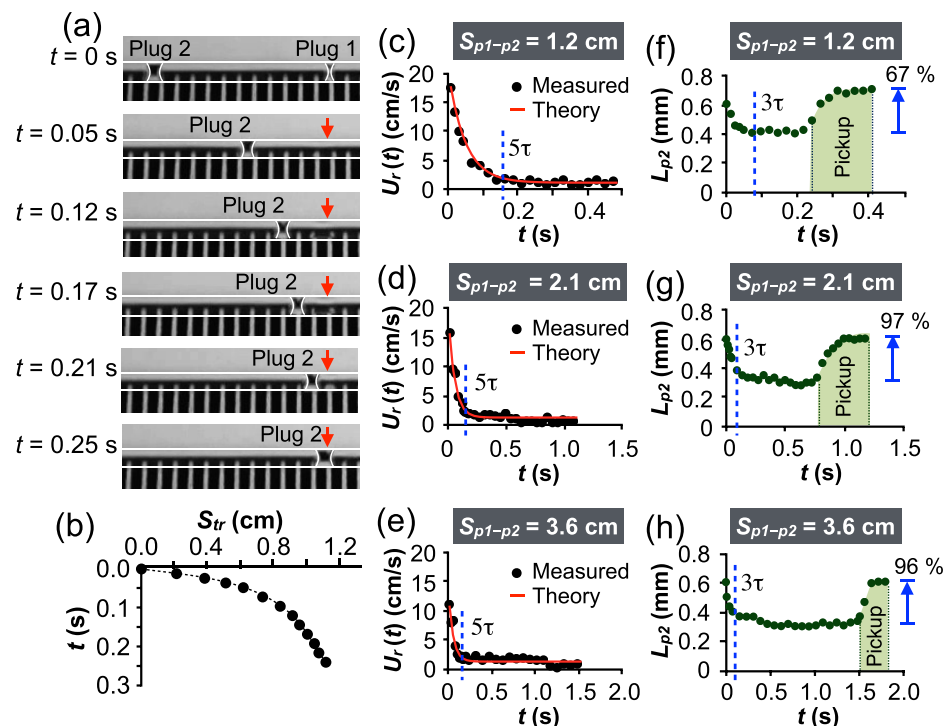


FIG. 4. Measurements of trajectory, travel speed, and length change of Plug 2 during retraction. (a) Time-lapse images and (b) trajectory of Plug 2 in a capillary tube. Arrows indicate the location where Plug 1 ruptured. Each grid is 1 mm. (c)–(e)  $U_r(t)$  and (f)–(h)  $L_{p2}$  of Plug 2 measured for different  $S_{p1-p2}$ . Theoretically obtained plug retraction speeds: (c)  $U_r(t) = 15.8e^{-t/0.03} + 1.2$ , (d)  $U_r(t) = 14.8e^{-t/0.03} + 1.2$ , and (e)  $U_r(t) = 9.8e^{-t/0.03} + 1.2$ .

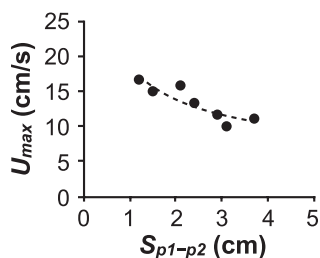


FIG. 5.  $U_{max}$  of Plug 2 measured against various  $S_{p1-p2}$  during plug retraction in a glass capillary ( $r = 450 \mu\text{m}$ ).

shows that at the very beginning of plug retraction  $U_r(t \approx 0) = U_{max} = 17 \text{ cm/s}$ , and the plug slowed down to  $U_f = 1.2 \text{ cm/s}$  in about  $5\tau = 1.5 \text{ s}$ , where  $\tau = 0.03 \text{ s}$ . Therefore, we obtained  $U_r(t) = (U_{max} - U_f)e^{-t/\tau} + U_f = 15.8e^{-t/0.03} + 1.2$ . Similarly, we determined that  $U_r(t) = 14.8e^{-t/0.03} + 1.2$  and  $U_r(t) = 9.8e^{-t/0.03} + 1.2$  for  $S_{p1-p2} = 2.1 \text{ cm}$  and  $3.6 \text{ cm}$ , respectively, as shown in Figs. 4(d) and 4(e). In all cases, the measured and calculated plug speeds correspond well with each other.

As shown in Figs. 4(f)–4(h),  $L_{p2}$  decreased faster at the beginning of plug retraction ( $t < 3\tau \sim 0.09 \text{ s}$ ) in all cases. However, changes in  $L_{p2}$  became unnoticeable as the plug slowed down due to viscous resistance. When Plug 2 approached the point of rupture of Plug 1,  $L_{p2}$  started to slowly increase as the plug picked up the residual volume of Plug 1 (i.e., the liquid collar of Plug 1). Due to the volume pickup,  $L_{p2}$  increased by 67%, 97%, and 96%, respectively, at  $S_{p1-p2} = 1.2 \text{ cm}$ ,  $2.1 \text{ cm}$ , and  $3.6 \text{ cm}$  compared with the shortest  $L_{p2}$  during the retraction.

We also used high-speed imaging to verify that  $U_{max}$  of Plug 2 is strongly affected by plug interdistance  $S_{p1-p2}$ . For  $S_{p1-p2} = \sim 1\text{--}4 \text{ cm}$ ,  $U_{max}$  in a tube ( $r = 450 \mu\text{m}$ ) was measured. Figure 5 shows  $U_{max}$  at  $t = \sim 0.01 \text{ s}$  measured immediately after rupture of Plug 1. Consistent with the results of  $dU_r$  shown in Figs. 2(b) and 2(e),  $U_{max}$  increased with decreasing  $S_{p1-p2}$  because surface tension and  $L_c$  are inversely related, as shown previously by  $U_{max} \sim [(\sigma/L_c + P_r)/\rho]^{1/2}$ .

In this letter, we report experimental and theoretical studies of the rapid plug retraction of a series of water plugs traveling in a glass capillary tube. When the leading of two plugs ruptured, the speed of the lagging plug increased very rapidly to  $U_{max} \sim [(\sigma/L_c + P_r)/\rho]^{1/2}$  by surface tension and airflow. Due to viscous resistance, the speed of the plug decreased during plug retraction as  $U_r(t) = (U_{max} - U_f)e^{-t/\tau}$

+  $U_f$ . Our experimental results showed that  $U_{max}$  was inversely related to  $S_{p1-p2}$  and  $r$ , while it increased with  $Ca_p$ , which was consistent with theory. In addition,  $dU_r$  became smaller as  $Vol_{p2}$  increased because of the increasing effect of gravity. Interestingly, as the lagging plug continued to advance, the plug became larger as it picked up the volume of the liquid collar left by the rupture of Plug 1. We envision that these insights could lead to a better understanding of the transport of liquid plugs in small-scale, confined volumes such as porous media,<sup>20</sup> capillary channel networks,<sup>21,22</sup> and pulmonary conducting airways.<sup>8,9,23</sup>

The authors gratefully acknowledge the financial support of the NIH (Grant Nos. HL120046 and EB002520 to G.V.N.), the Sackler Foundation (pilot grant to J.K.), and the Mikati Foundation (to G.V.N.).

- <sup>1</sup>I. H. Shames, *Mechanics of Fluids* (McGraw-Hill New York, 1982).
- <sup>2</sup>J. B. Keller and M. J. Miksis, *SIAM J. Appl. Math.* **43**(2), 268 (1983).
- <sup>3</sup>M. Prakash, D. Quéré, and J. W. Bush, *Science* **320**(5878), 931 (2008).
- <sup>4</sup>D. Okawa, S. J. Pastine, A. Zettl, and J. M. Fréchet, *J. Am. Chem. Soc.* **131**(15), 5396 (2009).
- <sup>5</sup>C. Song, J. K. Moon, K. Lee, K. Kim, and H. K. Pak, *Soft Matter* **10**(15), 2679 (2014).
- <sup>6</sup>N. R. Morrow and G. Mason, *Curr. Opin. Colloid. Interface* **6**(4), 321 (2001).
- <sup>7</sup>J. Cai, X. Hu, D. C. Standnes, and L. You, *Colloid. Surface. A* **414**, 228 (2012).
- <sup>8</sup>M. Baudoin, Y. Song, P. Manneville, and C. N. Baroud, *Proc. Natl. Acad. Sci. USA* **110**(3), 859 (2013).
- <sup>9</sup>Y. Song, M. Baudoin, P. Manneville, and C. N. Baroud, *Med. Eng. Phys.* **33**(7), 849 (2011).
- <sup>10</sup>M. Mall, B. R. Grubb, J. R. Harkema, W. K. O'Neal, and R. C. Boucher, *Nat. Med.* **10**(5), 487 (2004).
- <sup>11</sup>D. F. Rogers and P. J. Barnes, *Ann. Med.* **38**(2), 116 (2006).
- <sup>12</sup>F. Bretherton, *J. Fluid. Mech.* **10**(02), 166 (1961).
- <sup>13</sup>L. Landau and B. Levich, "Dragging of a Liquid by a Moving Plate," *Acta Physicochim URSS* **17**, 42–54 (1942).
- <sup>14</sup>G. K. Batchelor, *An Introduction to Fluid Dynamics* (Cambridge University Press, 2000).
- <sup>15</sup>K. B. Glasner, *SIAM J. Appl. Math.* **69**(2), 473 (2008).
- <sup>16</sup>K. Glasner, F. Otto, T. Rump, and D. Slepčev, *Eur. J. Appl. Math.* **20**(01), 1 (2009).
- <sup>17</sup>F. Culick, *J. Appl. Phys.* **31**(6), 1128 (1960).
- <sup>18</sup>C. Lv, C. Clanet, and D. Quéré, *J. Fluid. Mech.* **778**, R6 (2015).
- <sup>19</sup>M. J. Fuerstman, A. Lai, M. E. Thurlow, S. S. Shevkoplyas, H. A. Stone, and G. M. Whitesides, *Lab Chip* **7**(11), 1479 (2007).
- <sup>20</sup>G. Dagan, *Flow and Transport in Porous Formations* (Springer-Verlag GmbH & Co. KG., 1989).
- <sup>21</sup>C. N. Baroud, S. Tsikata, and M. Heil, *J. Fluid. Mech.* **546**, 285 (2006).
- <sup>22</sup>D. P. Gaver III, R. W. Samsel, and J. Solway, *J. Appl. Physiol.* **69**(1), 74 (1990).
- <sup>23</sup>J. B. Grotberg, *Phys. Fluids* **23**(2), 021301 (2011).